

Thermal pressurization during “slip law” frictional earthquake nucleation

STUART V. SCHMITT and PAUL SEGALL  Department of Geophysics, Stanford University

INTRODUCTION

For decades, researchers have considered shear heating-induced thermal pressurization as a potential dynamic weakening mechanism during earthquakes. In this hypothesis, shear heating pressurizes the pore fluid faster than it can diffuse away, thereby reducing the effective normal stress on the fault.

Segall & Rice [2006] suggested that thermal effects may become dominant during the quasi-static nucleation phase, which is usually modeled using isothermal rate- and state-dependent friction. Using the simple slip history predicted by “aging law” rate/state friction—along with reasonable estimates of heat and pore pressure transport parameters—they estimated that thermal pressurization dominates frictional weakening at slip rates in excess of 10^{-5} to 10^{-3} m/s.

In the last few years, we have explored that problem further by performing numerical simulations of earthquake nucleation using fully coupled elasticity, friction, and heat/fluid transport. We confirmed the Segall-Rice [2006] hypothesis and observed an interesting behavior in the nucleation zone—that the nucleation zone shrinks as slip accelerates.

Thermal pressurization is effectively a slip weakening mechanism that feeds back into itself, and therefore rapidly dominates in the center of an aging law nucleation zone, where the most slip occurs. This effect leads to dramatic along-strike localization of the nucleation zone at its midpoint (see Figure 1).

With the slip (logarithmic) friction evolution law, however, nucleation is pulslike. That is, the fastest-slipping portion of the nucleation zone propagates unidirectionally, with velocity decaying behind [Ampuero & Rubin, JGR, 2008]. Under this regime, the relative importance of thermal pressurization is diminished since most of the frictional weakening occurs in locations with limited amounts of slip. In the present work, we explore in detail the effect of thermal pressurization on slip law earthquake nucleation.

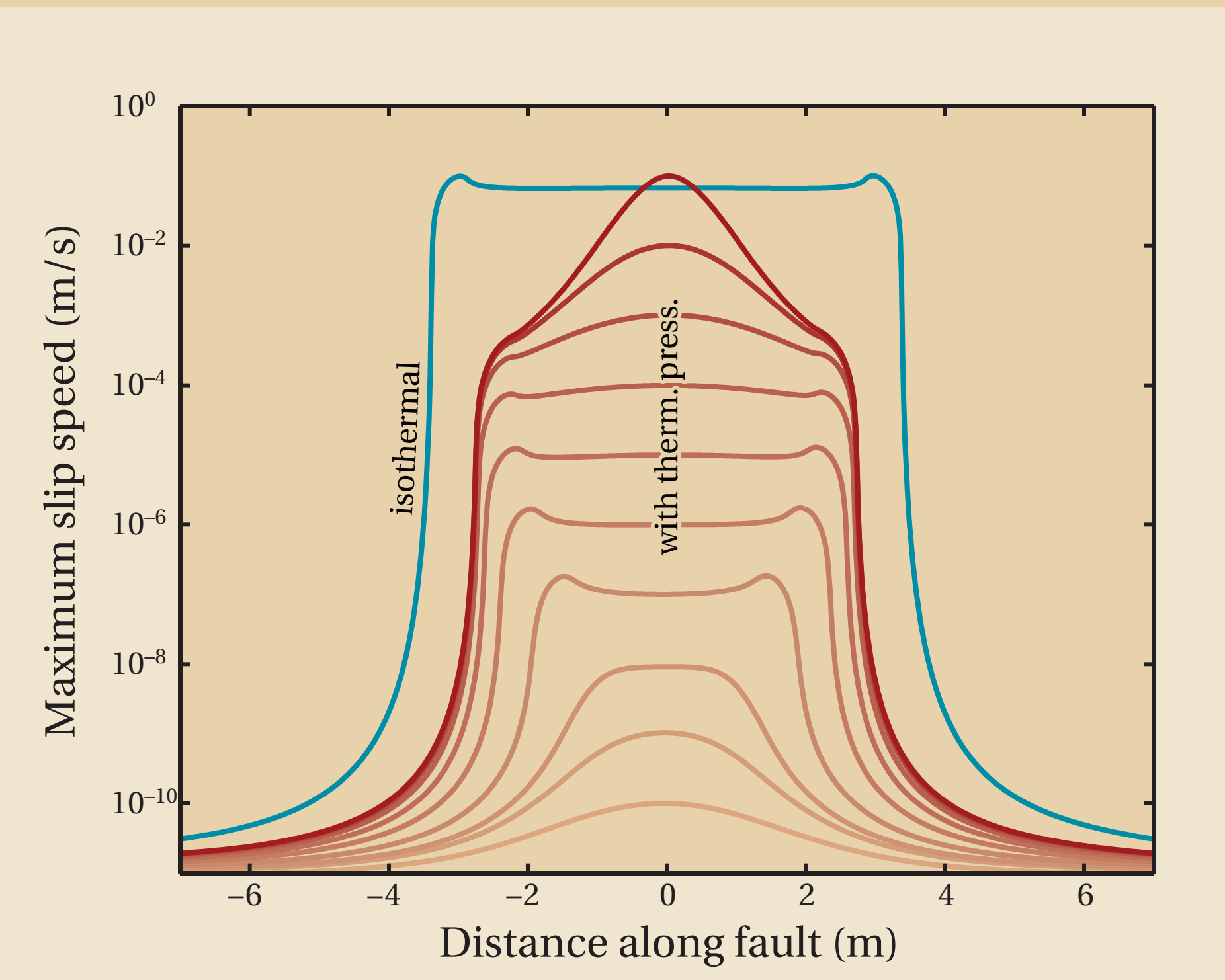


Figure 1. The effect of thermal pressurization on aging law nucleation. Lines are snapshots of slip speed on the fault. In red, snapshots for every 10-fold increase in v_{\max} are shown for nucleation with thermal pressurization. The nucleation zone starts as a growing crack, then shrinks. For comparison, the isothermal profile for $v_{\max} = 10^{-1}$ m/s is shown; crack growth continues in this case.

GOVERNING EQUATIONS, CONTINUED

If the thermal and hydraulic transport properties are uniform, then the pore pressure and temperature change on the fault are uniquely related through [Rice, 2006]

$$\Delta p(y=0) = \frac{\Lambda}{1 + \sqrt{c_{\text{hyd}}/c_{\text{th}}}} \Delta T(y=0). \quad (8)$$

C. When is thermal pressurization important?

The time derivative of (3) is

$$\frac{d\tau_{\text{fric}}}{dt} = \underbrace{\frac{d\mu}{dt}(\sigma - p_0)}_{\text{friction}} - \underbrace{\mu_0 \frac{dp}{dt}}_{\text{thermal pressurization}}. \quad (9)$$

We define the critical velocity v_{crit} to be when the thermal pressurization term in (9) is larger than the friction term in the area of the fault that has undergone any sort of weakening.

Table of parameters

G	shear modulus	10 GPa
v_s	s-wave velocity	3700 m/s
μ_0	nominal friction	0.6
α	coeff. of σ effect on θ	0.6
a	friction velocity effect	0.015
b	friction state effect	0.019
d_c	slip weakening distance	100 μm
c_{th}	thermal diffusivity	10^{-6} m ² /s
c_{hyd}	hydraulic diffusivity	10^{-6} m ² /s
ρc_p	density \times heat capacity	2.86 MPa/ $^{\circ}\text{C}$
Λ	thermal coupling param.	0.8 MPa/ $^{\circ}\text{C}$
θ	friction state	
v	slip speed	
T	temperature (change)	
p	pore pressure (change)	
σ	normal stress	
λ_p	pore fluid expansivity	
β_p	pore fluid compressibility	
β_p	pore fluid compressibility	

RESULTS

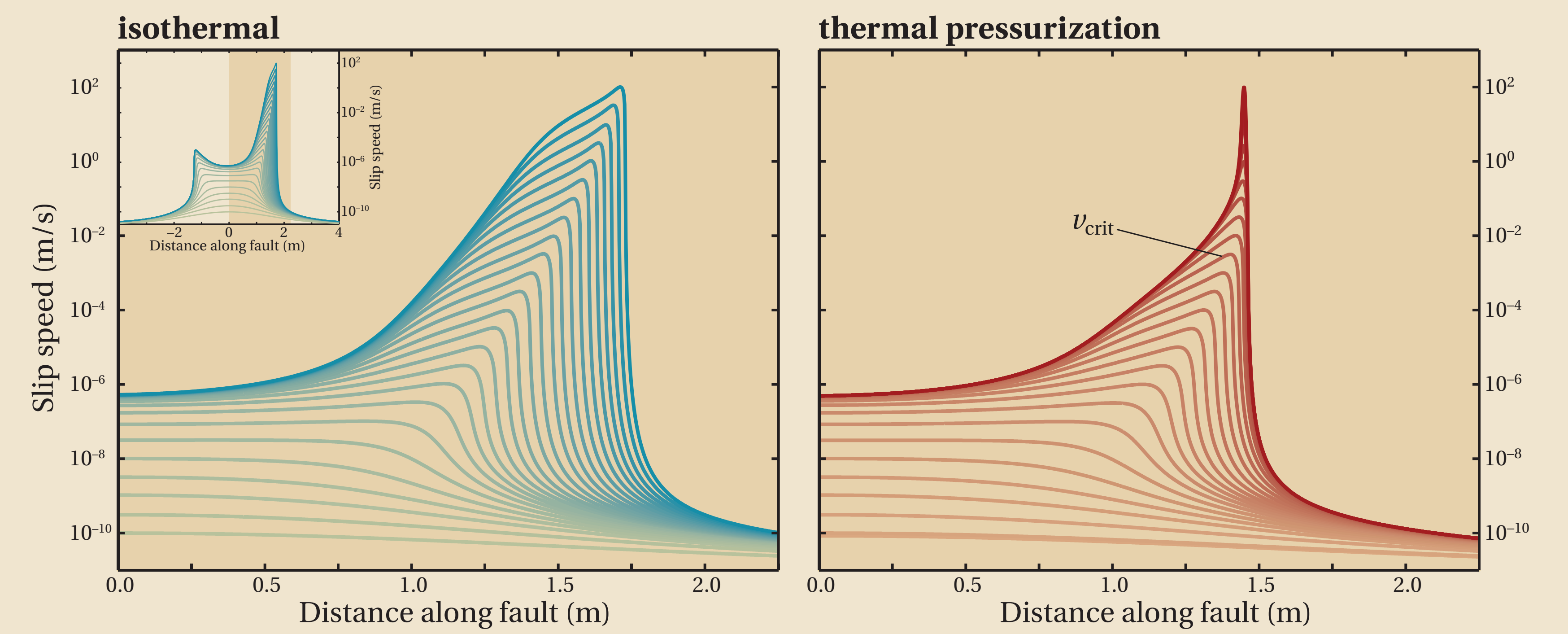


Figure 3. Comparison of slip law nucleation: isothermal (left, blue) and with thermal pressurization (right, red). The snapshots selected here and in subsequent figures are shown on the curve to the lower right. Bolder colors indicate later time. Both simulations shown here were started with identical initial conditions, using parameters shown in the table above (but with radiation damping turned off for clarity).

Isothermal slip law nucleation is pulslike (here, moving rightward), with slip speed decaying behind the pulse tip. The pulse shape is somewhat self-similar, if scaled by $\ln(v_{\max})$.

With thermal pressurization, nucleation starts out in the same manner as the isothermal case. After thermal pressurization dominates, however, the pulse width contracts.

In the slip speed-time curve at right, note that thermal pressurization has only slightly advanced the time of the earthquake.

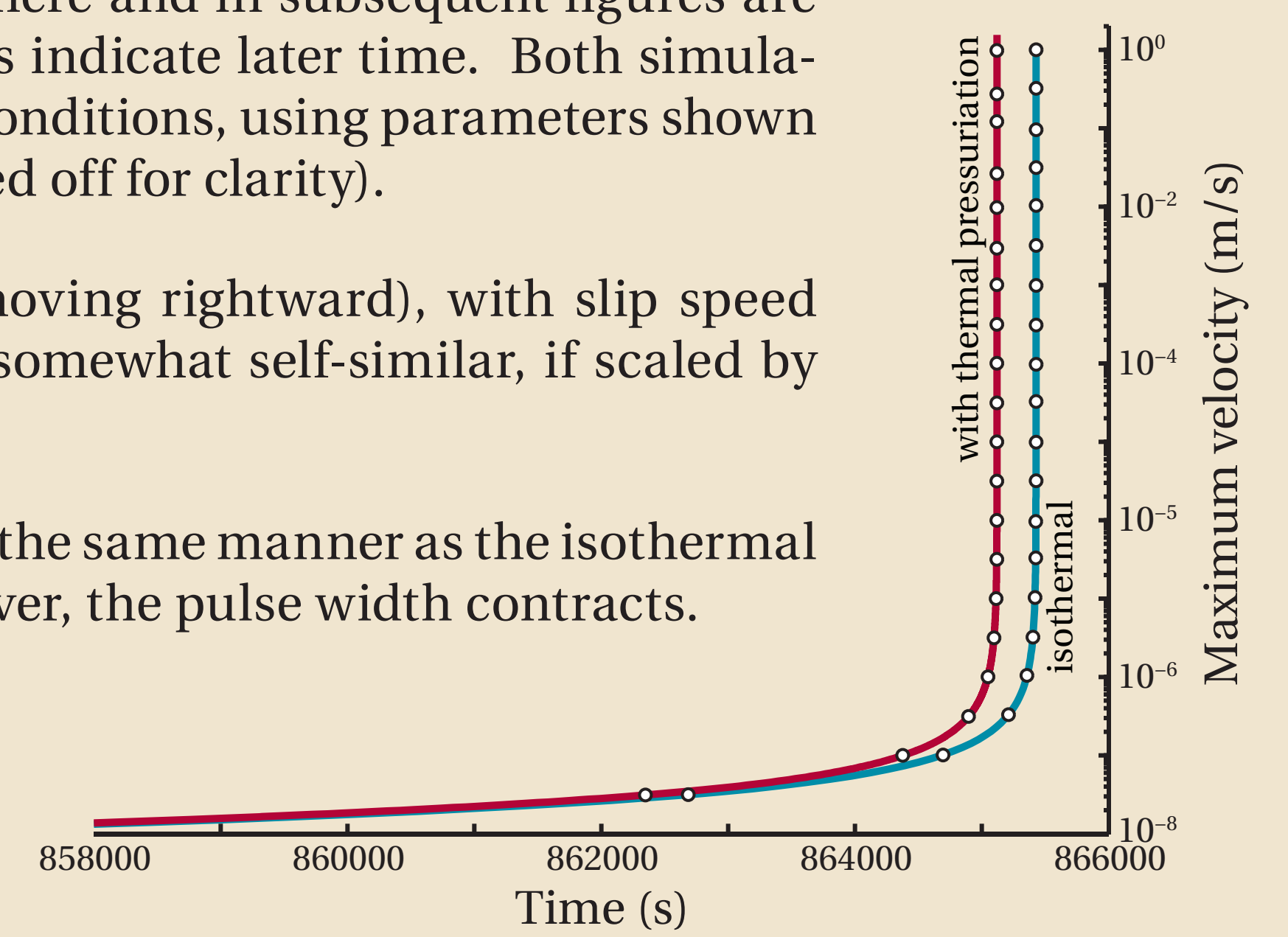


Figure 4. Critical velocity v_{crit} . The two terms in eq. (9) are plotted against v_{\max} . Rate-state friction dominates the weakening until $v_{\text{crit}} = 0.005$ m/s, at which point thermal pressurization becomes the dominant weakening term in the equation of motion.

By the time $v_{\max} = 0.02$ m/s, thermal pressurization becomes the *only* weakening term. Rate-state friction becomes strengthening because of its direct velocity strengthening component (the a term in eq. [3]).

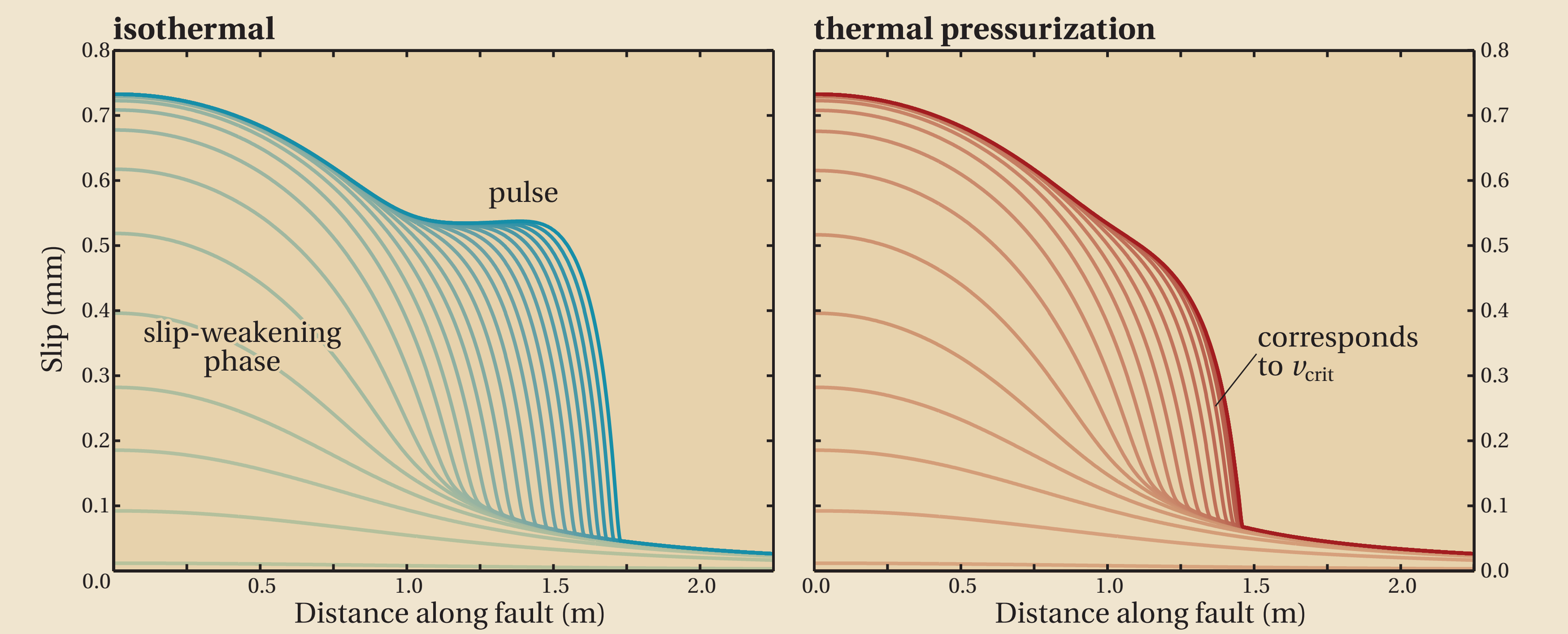


Figure 5. Cumulative slip; snapshots correspond to those shown in Figure 3. In isothermal nucleation, the initial slip-weakening phase is clearly followed by a propagating pulse. With thermal pressurization, the pulse starts in an identical manner. After v_{crit} is attained, however, it does not travel as far for corresponding values of v_{\max} .

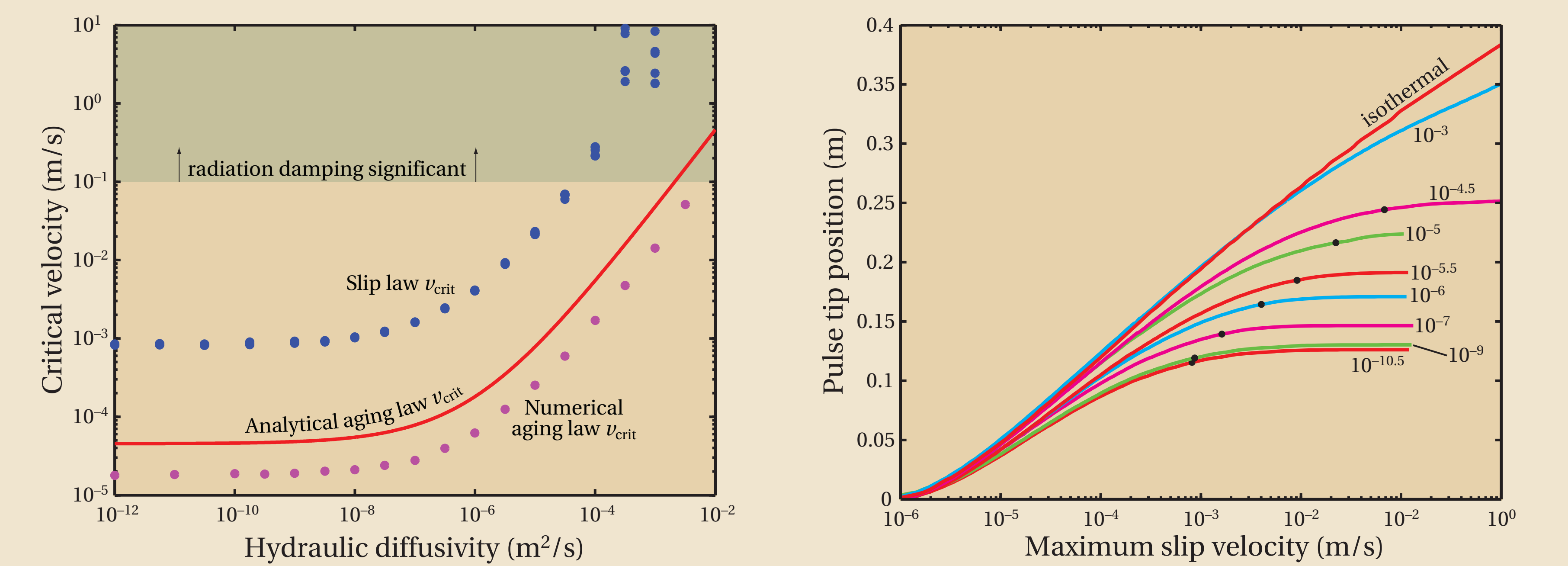


Figure 6. The effect of hydraulic diffusivity c_{hyd} —the least well-known parameter—on thermal pressurization.

In the left plot, we present the dependence of v_{crit} on c_{hyd} . For the parameters used here, thermal pressurization dominates before seismic radiation for $c_{\text{hyd}} < 10^{-5}$ m²/s. The values of slip law v_{crit} are consistently ~40 times greater than those for aging law nucleation. The analytical prediction of Segall & Rice [2006] for the aging law is also shown.

In the right plot, we show how thermal pressurization affects the pulse propagation speed. Lines show how pulse tip position relates to v_{\max} for several values of c_{hyd} , with black dots showing v_{crit} . When $v_{\max} \approx 100v_{\text{crit}}$, the pulse effectively stops moving. Decreasing c_{hyd} , which promotes thermal pressurization, shortens the distance the pulse tip can travel.

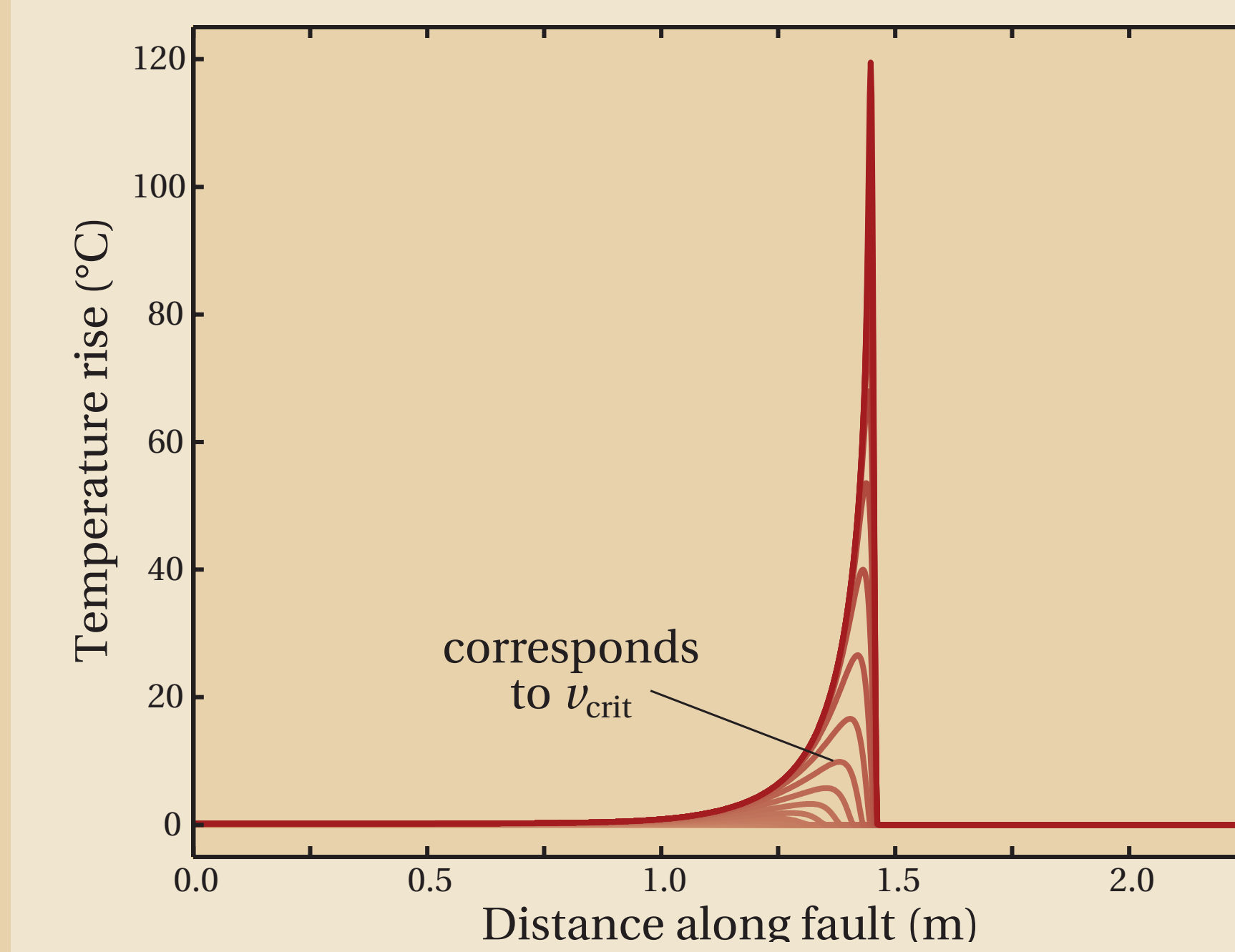
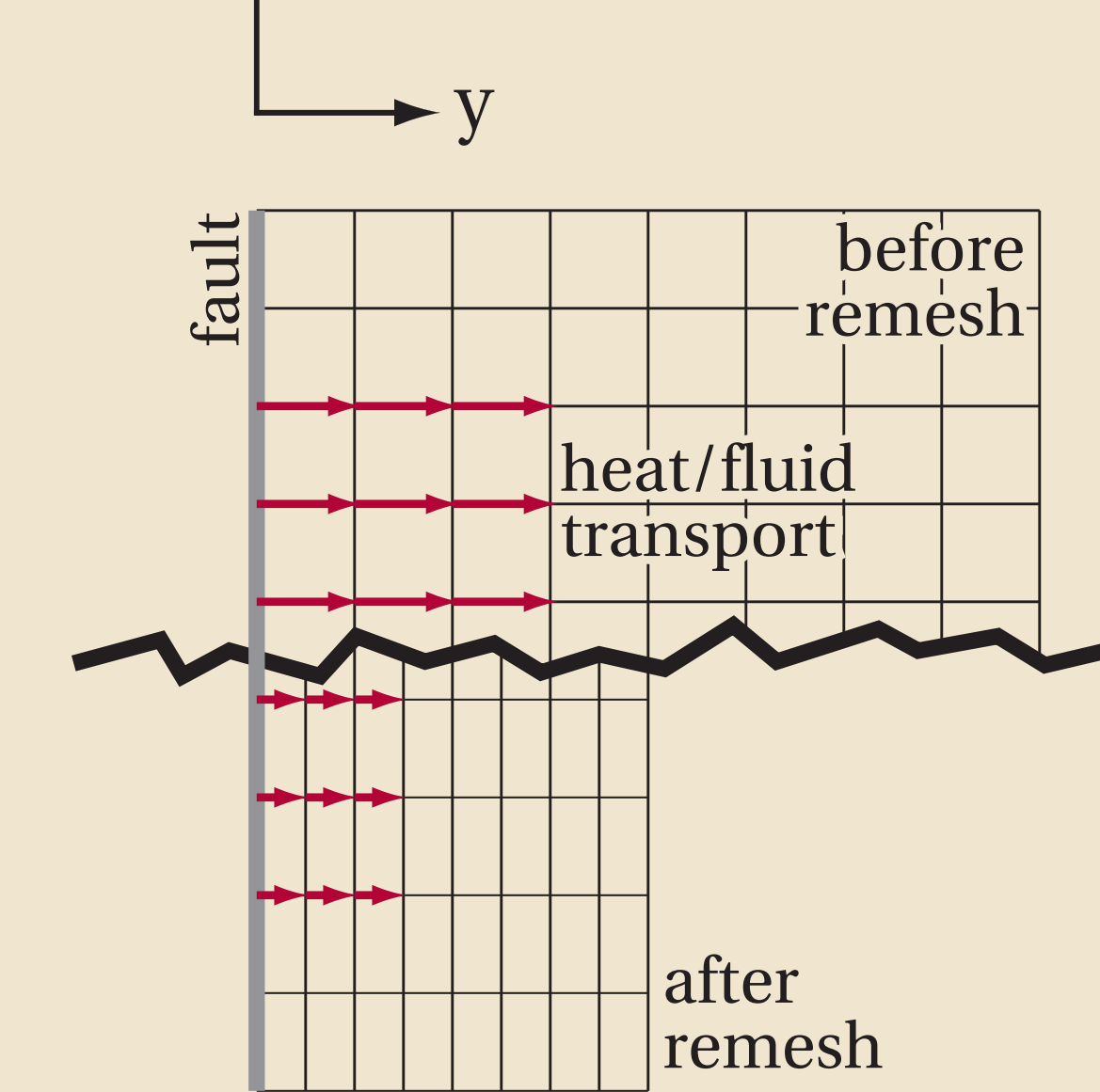


Figure 7. Snapshots of temperature rise on the fault. The 10 $^{\circ}\text{C}$ temperature rise corresponding to v_{crit} is modest but is an order of magnitude larger than $T(v_{\text{crit}})$ for the aging law.

CONCLUSIONS

- For reasonable values of material properties, thermal pressurization dominates frictional nucleation—either aging law or slip law—before the onset of seismic radiation.
- Thermal pressurization is delayed with slip law friction compared with aging law friction.
- The width of the nucleation zone shrinks after thermal pressurization dominates. Both aging law “cracks” and slip law “pulses” shrink.
- Thermal pressurization slows the propagation of nucleation pulses.
- By the time an earthquake ruptures dynamically, the nucleation zone may be a narrow, stationary feature.

Figure 2. Schematic of model



DESCRIPTION OF MODEL

- 2D finite difference diffusion grid.
- Shear heating included as a boundary condition.
- Diffusion away from fault only.
- Grid refinement as accuracy demands.
- Stress rate and slip rate related through a Hilbert transform in the Fourier domain.
- Driven by constant remote stress rate.
- Started below steady state ($v\theta/d_c < 1$), with a small span at slightly higher v to influence location of nucleation.

GOVERNING EQUATIONS

A. Shear stress on the fault

Elastic stress interaction:

$$\tau_{\text{el}}(x) = -\frac{G}{2\pi} \int_{-\infty}^{\infty} \frac{1}{x-\xi} \frac{\partial u}{\partial \xi} d\xi. \quad (1)$$

Radiation damping approximation [Rice, 1993]:

$$\tau_{\text{rad}} = \frac{G}{2v_s} v. \quad (2)$$

Rate- and state-dependent friction:

$$\tau_{\text{fric}} = \left[\mu_0 + a \ln \frac{v}{v_0} + b \ln \frac{\theta v_0}{d_c} \right] \sigma_{\text{eff}}. \quad (3)$$

with the slip state evolution law and Linker-Dieterich [1992] effect (necessary to regularize the problem):

$$\frac{d\theta}{dt} = -\frac{\theta v}{d_c} \ln \frac{\theta v_0}{d_c} - \frac{\alpha \theta}{b \sigma_{\text{eff}}} \frac{d\sigma_{\text{eff}}}{dt}. \quad (4)$$

Together, (1)–(4) form the equation of motion

$$\tau_{\text{el}} - \tau_{\text{fric}} - \tau_{\text{rad}} = 0. \quad (5)$$

We numerically integrate the time derivative of (5) to determine v , θ , p , and T .

B. Generation/transport of heat and pore pressure

Thermal diffusion and shear heating on the fault:

$$\frac{\partial T}{\partial t} = c_{\text{th}} \frac{\partial^2 T}{\partial y^2} \quad \text{and} \quad \frac{\partial T}{\partial y} \Big|_{y=0} = -\frac{\tau v}{2\rho c_p c_{\text{th}}}. \quad (6)$$

Pore pressure generation and transport:

$$\frac{\partial p}{\partial t} = c_{\text{hyd}} \frac{\partial^2 p}{\partial y^2} + \Lambda \frac{\partial T}{\partial t} \quad \text{with} \quad \Lambda = \frac{\lambda_f - \lambda_\phi}{\beta_f + \beta_\phi}. \quad (7)$$